meridian are included, the rate is reduced to 13.04° per day and the standard error is increased to 0.18° per day.

At low altitudes the nonlinearity of atmospheric refraction introduces a slight vertical distortion in the solar image. At a true (geometric) altitude of 1° a spot that is actually at the center of the solar disk would appear 5″ below the midpoint of the apparent vertical diameter, based on an interpolation equation fitted to the refraction tabulated by Allen (*10*). Incidentally, the apparent altitude of the sun's center would be 1°22′ and the vertical diameter would appear compressed by 10 percent, but these large effects would not cause systematic errors in spot positions because of my allowance for linear distortion on the drawings. Although the nonlinear effect is small, the altitude-dependent correction equations, once written to check the significance of refraction, were retained in the reduction program.

Systematic errors originating in Harriot's technique, particularly those that would result in a reduced rotation rate, are a major concern but are very difficult to reconstruct. The perceptual phenomenon of irradiation could cause him to draw the sun too large depending on the image brightness. If, for example, he systematically drew the sun 2 percent too large, the corrected rotation rate would be 13.73° ± 0.10° (standard error of the mean) per day. A test assuming the sun to be 3 percent smaller than drawn failed because this put some spots off the limb. Any systematic errors resulting from telescopic distortions have probably been broken up into random errors because only a part of the sun could be seen in the field, so that scanning was required. Also, various telescopes were used.

Harriot's careful plotting of spot positions is evident from the fact that the average value for the standard deviation of a spot about its computed mean latitude was only 3.2°. It is difficult to escape the conclusion that the sun's rotation, as defined by sunspots, was truly slow at the time Harriot observed it, and that it was accelerating between then and the inception of the Maunder minimum.

RICHARD B. HERR

Department of Physics and Astronomy, University of Delaware, Newark 19711

References and Notes

1. J. A. Eddy, *Science* **192**, 1189 (1976); *Sci. Am.* **236** (No. 5), 80 (1977).
2. _____, P. A. Gilman, D. E. Trotter, *Science* **198**, 824 (1977).
3. England was still using the Julian calendar in Harriot's time. The equivalent dates in the Gregorian calendar (for example, to compare with Galileo's observations) are 11 December 1611 through 28 January 1613.
4. Harriot's original sunspot drawings are the possession of Lord Egremont and Leconfield and are retained at Petworth House, Sussex, where they were taken on Harriot's death in 1621. Photocopies of them may by seen at the Bodleian Library at Oxford and the Science Museum in South Kensington, London. In this country, a complete set of Harriot photocopies may be viewed in the History of Science Library of the University of Delaware. I worked from the Delaware copy of HMC 241/8, kindly lent me by J. W. Shirley.
5. J. North, in *Thomas Harriot, Renaissance Scientist*, J. W. Shirley, Ed. (Clarendon, Oxford, 1974), pp. 129–165. The prevailing use of the early Dutch or "Galilean" telescope at the beginning of the 17th century and its field of view are discussed on pp. 144–149 and 158–160. In footnote 55, North suggests that the unnumbered duplicate of the 11 August 1612 drawing could be the original made at the telescope.
6. Baron de Zach remarks on the assertion that Thomas Harriot "had the custom of holding the mathematical brass instruments, when working, in his mouth." A translation of his 1788 paper was reprinted in S. P. Rigaud, *Supplement to Dr. Bradley's Miscellaneous Works with an Account of Harriot's Astronomical Papers* (Oxford, 1833), pp. 57–61.
7. B. Tuckermann, *Planetary, Lunar, and Solar Positions A.D. 2 to A.D. 1649 at Five-day and Ten-day Intervals* (American Philosophical Society, Philadelphia, 1964).
8. R. C. Carrington, *Observations on the Spots on the Sun from November 9, 1853 to March 24, 1861, Made at Redhill* (Williams and Norgate, London, 1863), as cited in J. A. Eddy, P. A. Gilman, D. E. Trotter. *Sol. Phys.* **46**, 3 (1976).
9. A sidereally fixed reference point—the great circle passing through the adopted rotational pole and the ecliptic pole—was used to define "longitude". This is not the heliographic longitude whose reference point rotates with the sun.
10. C. W. Allen, *Astrophysical Quantities* (Athlone, London, ed. 3, 1973), p. 183; refraction tables are on p. 125.
11. F. Ward, *Astrophys. J.* **145**, 416 (1966).
12. H. Wöhl, *Astron. Astrophys.* **62**, 165 (1978).
13. I thank D. J. Mullan for helpful discussions, M. P. Raphael for assistance in selecting spots and for measuring them on the digitizer, and the University of Delaware Computing Center for a grant of computer time. I especially thank J. W. Shirley, who introduced me to the work of Thomas Harriot and whose enthusiastically shared knowledge of Harriot was an invaluable resource.

5 April 1978; revised 27 June 1978

Sieve Areas in Fossil Phloem

Abstract. *Phloem tissue of the Pennsylvanian fern* Etapteris *is described from permineralized specimens. Sieve elements possess regularly aligned sieve areas containing pores on the radial walls. The presence of these structures provides a basis for comparison with the phloem of living ferns.*

Vascular plants are characterized by the presence of two principal tissues that make up the conducting system. Xylem is involved in the conduction of water, whereas phloem is responsible for the movement of solutes, principally sugars, in the plant. The basic cell of the phloem tissue is an elongate, thin-walled cell termed the sieve element, which is characterized by the presence of perforations in the walls. These sieve pores are usually aggregated into definite regions on the cell wall that are termed sieve areas. The presence of sieve areas provides the basis for recognition of sieve elements in vascular plants.

The identification of phloem tissue is rare in studies of fossil plants. The features used to determine extant phloem cells are rarely encountered in the fossil record because of the delicate nature and hence the poor preservation of thin-walled phloem cells (*1, 2*). Consequently, the recognition of fossil phloem is limited to the position these cells occupy in the axis and the identification of sieve areas on the cells. In addition, because of the relatively small size of the cells, their presence in a mineral matrix, and the resolution limits imposed by light microscopy, little information has been obtained to date about the histology of fossil phloem.

This study was performed to describe the structure and occurrence of phloem cells in petiole segments of the Carboniferous fern *Etapteris leclercqii* (*3*) that are preserved in calcium carbonate permineralizations (coal balls). The specimens were collected at the Lewis Creek locality in eastern Kentucky and are stratigraphically associated with the Magoffin marine zone. Although there is some dispute regarding the precise position of these deposits in the Pennsylvanian System, the floral elements clearly suggest that the sediments are of Lower Pennsylvanian age (*4*).

Specimens were prepared for light microscopy by using the cellulose acetate peel technique, and for scanning electron microscopy (SEM) by etching the phloem zone in dilute hydrochloric acid (2 percent of the stock solution) for 10 minutes followed by immersion in saturated EDTA for 8 minutes. After drying, the specimens were mounted on standard SEM stubs with double stick tape, and sputter-coated with approximately 100 Å of gold. The radial walls of the sieve elements were examined at 20 kV in the secondary emission mode.

Figure 1A illustrates a transverse section of the petiole of *E. leclercqii*. The center of the axis is a core of xylem tracheids that in transverse section has the shape of an hourglass (clepsydroid). A zone of phloem tissue, approximately four cells wide, surrounds the xylem. Separating the xylem and phloem is a parenchyma sheath one to two cells wide that is visible in longitudinal section as uniform rectangular cells (Fig. 1, A and C). Crushed parenchyma cells that may

0036-8075/78/1208-1081$00.50/0

represent a pericycle or endodermis occur immediately outside the phloem. The remaining tissues of the petiole form a broad cortical zone. The presence of histological continuity from the xylem tracheids to the cortex provides direct evidence for the identification of a definite phloem zone in this fossil fern (Fig. 1, A and C).

The phloem of *Etapteris* is constructed entirely of sieve elements (*5*) up to 40 μm in diameter and 120 μm in length. End walls range from horizontal to distinctly oblique, with some cells exhibiting the swollen ends that have often been observed in the sieve elements of extant ferns (Fig. 1B). In transmitted light the radial walls characteristically appear as discontinuous horizontal dark bands separated by lighter elliptical areas (Fig. 1F). Some of these regions that are confined to the radial walls undoubtedly represent sieve areas; others may be the result of differential light diffraction patterns through degraded cell wall material. Distinguishing sieve areas from such regions of degradation is extremely difficult since the sieve pore diameter often approaches the resolution limits of light microscopy. The sieve pore diameter in some extant vascular cryptogams may be as small as 0.05 to 0.07 μm (*6*).

Because of the size of the sieve elements in *Etapteris* it was necessary to examine cells for sieve areas with the aid of the SEM. The radial wall of a sieve element is illustrated in Fig. 1D, where the sieve areas appear as regularly spaced elongate depressions that are aligned perpendicular to the long axis of the cell. Sieve pores are similar in size and shape and are confined to these elliptical depressions (Fig. 1, E and G). Both depressions and associated pores have been observed only on the radial walls of sieve elements, and adjacent parenchyma cells exhibit no comparable structural complexities.

Fossil phloem has been described in Paleozoic representatives of several major plant groups including the arthrophytes, lycopods, seed ferns, and several problematic taxa (*7–9*). The oldest known occurrence of a probable phloem tissue was reported in the Devonian plant *Rhynia* (*10*). In addition to these reports of phloem in Paleozoic plants, well-preserved sieve elements exhibiting sieve areas have also been described from silicified Mesozoic plants (*11*). All of these reports are based solely on transmitted light studies, and most describe phloem cells in terms of their general morphology and their position in the axis. Relatively few of these reports document the existence of sieve areas. To date, primary phloem has been identified in only three fossil plant taxa, *Astromyelon*, *Lepidodendron*, and *Sphenophyllum* (*8*, *9*, *12*), and has not been described in any Paleozoic fern. Eggert and Kanemoto (*9*) describe elongate elliptical holes on the radial walls in the phloem of a *Lepidodendron* stem that they interpret as sieve areas. Scanning electron microscopy of similar wall configurations in *Etapteris* petioles suggests that these elliptical holes do in fact represent sieve areas that regularly contain pores.

Our present understanding of possible phylogenetic trends in specialization of

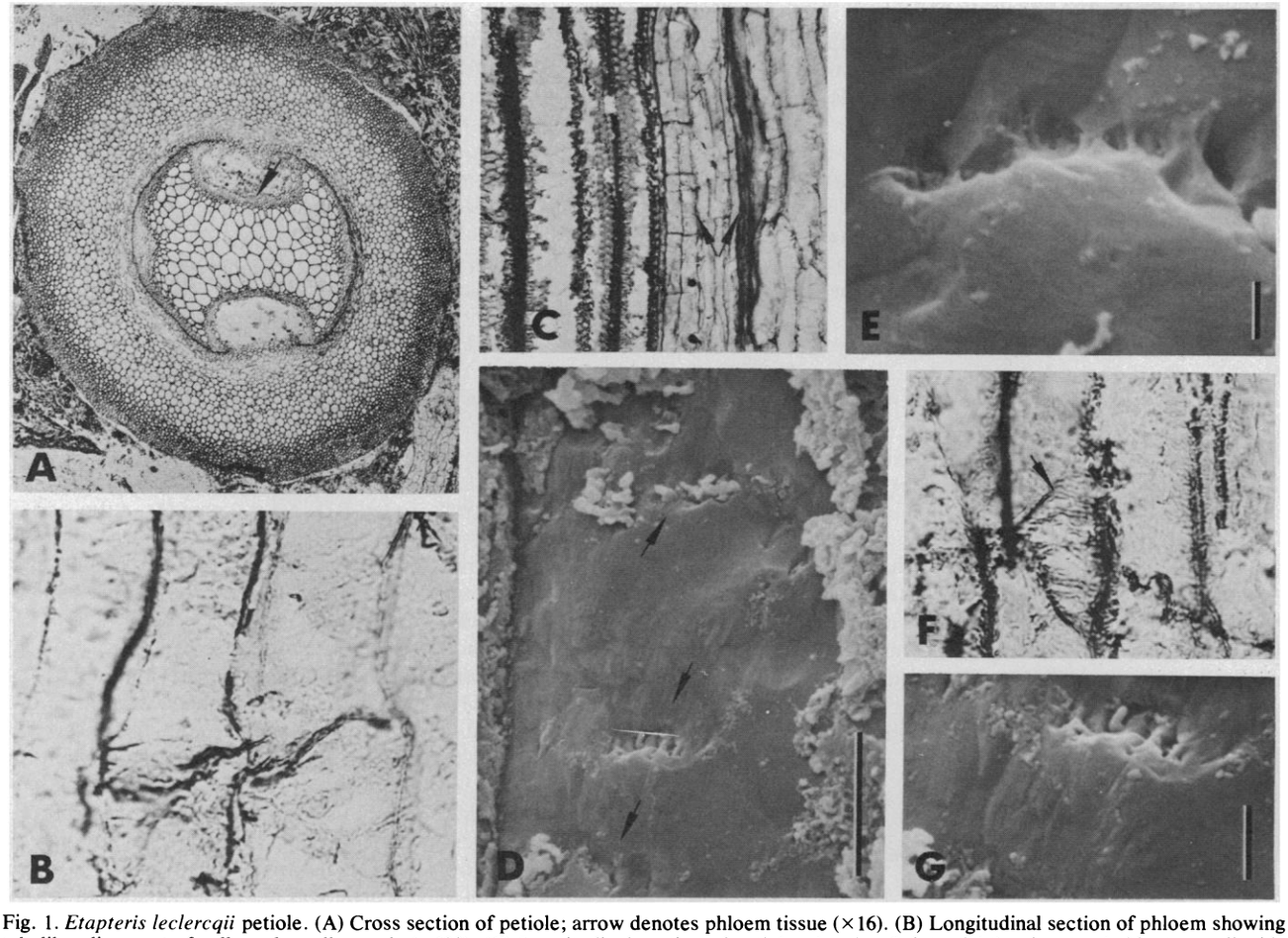

Fig. 1. *Etapteris leclercqii* petiole. (A) Cross section of petiole; arrow denotes phloem tissue (×16). (B) Longitudinal section of phloem showing tubelike alignment of cells and swollen ends (×600). (C) Longitudinal section of petiole, showing (left to right) xylem tracheids, two-cell-wide parenchyma sheath, phloem zone (between arrows), zone of crushed cells, and inner cortex (×150). (D) Radial wall of a sieve element, showing depressed horizontal sieve areas (arrows) (scale bar, 5 μm). (E) Close-up of sieve area showing sieve pores (scale bar, 1 μm). (F) Sieve element with possible sieve area (arrow) (×800). (G) Low-angle view of sieve area containing pores (scale bar, 1 μm).

phloem cells is based entirely on the histology of extant materials (*13*). This study provides a basis for the continued examination of vascular plant phloem in the fossil record, and suggests that additional refinement of paleobotanical techniques may lead to a greater understanding of phloem evolution.

EDITH L. SMOOT
THOMAS N. TAYLOR
Department of Botany, Ohio State University, Columbus 43210

References and Notes

1. Features used to distinguish extant phloem cells include organelle composition and ultrastructure and staining properties of the protoplast. See Esau (*2*) for further information.
2. K. Esau, *The Phloem* (Borntraeger, Berlin, 1969).
3. E. L. Smoot and T. N. Taylor, *Am. J. Bot.* **65**, 571 (1978).
4. C. W. Good and T. N. Taylor, *Palaeontology* **13**, 29 (1970).
5. The use of the general term sieve element conforms to the terminology of Esau (*2*, p. 9) and designates the basic cell type of the phloem tissue, which is involved in conduction of organic solutes in plants. See also the discussions of phloem terminology in M. Kruatrachue and R. F. Evert [*Am. J. Bot.* **61**, 253 (1974)] and J. W. Perry and R. F. Evert [*ibid.* **62**, 1038 (1975)].
6. R. R. Dute and R. F. Evert, *Am. J. Bot.* **64**, 421 (1977); R. D. Warmbrodt and R. F. Evert, *ibid.* **61**, 267 (1974).
7. C. B. Beck, *ibid.* **44**, 350 (1957); J. Galtier and C. Hébant, *C. R. Acad. Sci. Ser. D* **267**, 2257 (1973); J. W. Hall, *Am. Midl. Nat.* **47**, 763 (1952); S. E. Scheckler and H. P. Banks, *Am. J. Bot.* **58**, 737 (1971); *ibid.*, p. 874; M. L. Wilson and D. A. Eggert, *Bot. Gaz. (Chicago)* **135**, 319 (1974).
8. D. A. Eggert and D. D. Gaunt, *Am. J. Bot.* **60**, 755 (1973).
9. D. A. Eggert and N. Y. Kanemoto, *Bot. Gaz. (Chicago)* **135**, 102 (1977).
10. D. F. Satterthwait and J. W. Schopf, *Am. J. Bot.* **59**, 373 (1972).
11. C. G. K. Ramanujam and W. N. Stewart, *ibid.* **56**, 101 (1969).
12. M. L. Wilson and D. A. Eggert, *Bot. Gaz. (Chicago)* **135**, 319 (1974).
13. K. Esau, V. I. Cheadle, E. F. Gifford, *Am. J. Bot.* **40**, 9 (1953).
14. Supported by NSF grants DEB77-02239 and DEB-01714.

12 June 1978; revised 16 August 1978

Rapid Light-Induced Changes in Near Infrared Transmission of Rods in *Bufo marinus*

Abstract. *Rapid transient changes in axial transmission of near infrared light through the outer segments of retinal rods of* Bufo marinus *are induced by illumination. The reasons for these changes are not clear. The changes in optical transmission may be useful in the study of photoreceptor function. However, the study of photoreceptor functions through the use of indicator dyes may be confounded by the intrinsic light-induced changes of optical properties of the photoreceptor cells.*

Retinal rods of *Bufo marinus* exhibit rapid light-induced changes in optical transmission for wavelengths longer than 650 nm; these transmission changes are too large to be attributed to changes in the absorption of rhodopsin or its photoproducts. This finding is surprising because the absorbance of rhodopsin (*1*) falls to below 0.1 percent of its peak value at wavelengths longer than 650 nm, and decreases approximately tenfold for each additional 30-nm increase in wavelength (*2*). Moreover, in the vertebrate retina, all known photoproducts that can be measured on the time scale of our experiments have absorbance maximums at wavelengths shorter than the parent rhodopsin and have no apparent secondary peaks at longer wavelengths. Therefore, the bleaching of rhodopsin or its photoproducts could account for no more than a 0.1 percent change in optical transmission through the rods at 650 nm and no more than a 10^{-6} percent change at 870 nm.

We mounted the isolated retina of *B. marinus* receptor-side up in a transparent dish on the stage of a compound microscope; oxygenated Ringer's solution (*3*) flowed through the dish. Both the stimulus beam (used to elicit photoreceptor responses) and the measuring beam (used to determine optical transmission) were directed at the retina through the microscope condenser (*4*).

The image of one, or many, of the rods whose axes were aligned with the optical axis of the microscope was focused on a photodetector (*5*) by means of a microscope objective (*6*). The wavelength of the measuring beam was selected by means of an interference filter (*7*) and was chosen to be in the far red or near infrared, away from the peaks of the absorption spectra of rhodopsin and its photoproducts. The measuring beam bleached an insignificant fraction of the rhodopsin, for example, no more than 5 rhodopsin molecules per rod per second for an 870-nm light (*8*). The stimulus light was restricted to wavelengths between 365 and 625 nm by an interference cutoff filter. For some experiments, single rod outer segments were impaled with micropipettes (*3*). In these experiments the measuring beam was passed through an interference filter (660 nm) and was also used as the stimulus; it bleached 6.4×10^4 rhodopsin molecules per rod per second.

A brief stimulus induced a change in optical transmission for a long-wavelength measuring light (Fig. 1). Changes in transmission were observed when measurements were made with light passing either through an area of retina that contained many hundreds of rods (Fig. 1) or through only a single rod (Fig. 2). The time course of these changes in transmission differed from that of the receptor potential (Fig. 2). The transmission changes had an action spectrum that was consistent with the absorption spectrum of rhodopsin (*9*); these changes disappeared after all the rhodopsin had been bleached (Fig. 1).

The rapid light-induced changes in transmission have the following properties. They fail to occur shortly after the flow of perfusate is stopped (*10*). They occur in retinas bathed in perfusate to which 2 m*M* aspartate has been added; therefore, they do not depend upon the activity of the proximal retinal neurons (*11*) and must arise in the rods. They persist in perfusate low in Na^+ (*3*); therefore, they do not depend on light-induced changes of ionic fluxes across the plasma membranes of the rods. A change in birefringence (*12*) does not account for the transmission changes because they were not attenuated after both the residual polarization of the incident light and the polarization sensitivity of the photodetector were reduced (*13*). Also, the transmission changes were not observed when the retina was placed between crossed polaroids (*14*). However, the amplitude of the transmission changes varied inversely with the numerical apertures of both the condenser and the objective.

The waveform of the transmission changes depended on stimulus irradiance and had a long duration that sometimes exceeded 10 seconds. The latency of the change in transmission was inversely related to stimulus irradiance. The lowest values of irradiance [with, for example, a 4.2 neutral density (ND) filter in Fig. 1] elicited a slow transmission increase, whereas higher values also elicited a more rapid component, a transmission decrease (3.0, 2.4, and 1.8 ND in Fig. 1). Thus, the higher values of irradiance elicited biphasic changes (for example, 3.0 and 1.8 ND in Fig. 1) or more complicated waveforms (for example, 2.4 ND in Fig. 1). The apparent drift of the baseline (Fig. 1) is probably attributable to stimulation by the measuring beam itself. The drift was more rapid for measurements at 750 nm than at 850 or 870 nm and was not seen after all the photopigment was bleached.

In three experiments, we measured changes in optical transmission at both 870 and 750 nm for the same retinal

0036-8075/78/1208-1083$00.50/0